

TARGET STUDIES FOR THE FCC-ee POSITRON SOURCE

F. Alharthi^{*1}, L. Bandiera³, I. Chaikovska¹, R. Chehab¹, J. Diefenbach⁴, O. Khomyshyn⁵,
D. Klekots⁵, W. Lauth⁴, A. Mazzolari³, V. Mytrochenko⁶, S. Ogur¹, M. Romagnoni³,
P. Sievers², M. Soldani^{†3}, A.I. Sytov³, A. Ushakov¹, S. Wallon¹, Y. Zhao²

¹CNRS-IJCLab, Paris-Saclay U., Orsay, France

²CERN, Geneva, Switzerland

³INFN Ferrara, Ferrara, Italy

⁴Institute of Nuclear Physics, J. Gutenberg University Mainz, Mainz, Germany

⁵Taras Shevchenko National University of Kyiv, Kyiv, Ukraine

⁶NSC Kharkiv Institute of Physics and Technology, Kharkiv, Ukraine

Abstract

FCC-ee injector study foresees 3.5 nC electron and positron bunches with 200 Hz repetition and 2 bunches per linac pulse at 6 GeV extraction energy. Regarding the possible options of positron production, we retain both of the conventional amorphous target and the hybrid target options. The hybrid scheme uses an intense photon production by 6 GeV electrons impinging on a crystal oriented along a lattice axis. In such a way, it involves two targets: a crystal as a photon radiator and an amorphous target-converter. Therefore, to avoid early failure or damage of the target, the candidate materials for the crystal and conversion targets have started to be tested by using the intense electron beam at Mainzer Mikrotron in Germany by the end of 2021. By manipulating the beam intensity, focusing, and chopping, a Peak Energy Deposition Density in the tested targets could be achieved close to that generated by the electron/photon beam in the FCC-ee positron target. Radiation-damage studies of the crystal sample have been also performed allowing estimating the effect on the photon enhancement used in the hybrid positron source.

(PEDD) need to be well addressed. On one side, the conventional target where a single amorphous target made of pure metals such as tungsten, tantalum, titanium, or the alloys such as W-Re26, TaW2.5 are retained as an option to be the standalone positron converter. On the other side, the hybrid target consisting of a thin crystal followed by a thicker amorphous target is promising [3]. However, the primary electron beam impinging on the crystal may deteriorate the crystal structure due to the important Coulomb scattering on the nuclei. Above some threshold nuclei can be dislodged from their sites [4]. A critical incident particle density (Fluence) may be determined; above such fluence the crystal structure is affected; that corresponds to the radiation damages on the crystal. Within this report, we will focus on the beam tests started in MAInzer MIkrotron (MAMI) to study the PEDD both on the amorphous and crystal targets and the effects of a high fluence, i.e. the total electron density on the targets. In case of the crystal target, the goal is to reach the fluence values close and even larger than those reached in the SLAC experiment [5]. The main results gathered in this experiment are presented hereafter.

INTRODUCTION

The conceptual design of the Future Circular positron-electron Collider, the FCC-ee, has been continuously evolving [1]. The collective effects in the collider and the integration of the tunnel set boundaries have been studied, while the injectors were further optimized in order to meet and maintain the ~ 1.3 A stored beam at its Z-operation, which will collect physics for 5 years.

Amongst 4 operational stages to study Z , W , H bosons and $t\bar{t}$, Z-operation demands the highest e^- and e^+ charge flux, namely at the order of $10^{12} - 10^{13}$ particles per second for each species. Comparing this e^+ flux with the ever existing and designed colliders [2], the FCC-ee challenge would differ in terms of high linac repetition of 200 Hz with 2 bunches per RF pulse on the converter target.

The required bunch population is $\sim 3.5 \times 10^{10}$, therefore, the heat load as well as the Peak Energy Deposition Density

THE FCC-ee PRE-INJECTOR AND POSITRON SOURCE

The FCC collaboration has submitted the conceptual design report in December 2018 [1]. The project design of the FCC-ee has been continuously evolving to overcome the technological difficulties as well as to ensure the realization of the best achievable lepton collider [6]. Further optimization of the extremely high luminosities led to an improvement of the injectors in comparison with the earlier design [7]. The linac operation is increased to 200 Hz with 2 bunches per RF pulse. Furthermore, 4 bunches per RF pulse consisting of 2 e^+ followed by 2 e^- bunches are needed during positron beam delivery to collider. The first 2 e^+ bunches will be put into the DR and the subsequent 2 e^- bunches will hit the positron converter and the generated positrons will be injected into the DR after acceleration to 1.54 GeV by a linac. The layout of the positron pre-injector and positron source is presented in Fig. 1. To ensure high reliability of the positron source, conventional and hybrid targets are currently under

* alharthi@ijclab.in2p3.fr

† mattiasoldani93@gmail.com

Content from this work may be used under the terms of the CC BY 4.0 licence (© 2022). Any distribution of this work must maintain attribution to the author(s), title of the work, publisher, and DOI

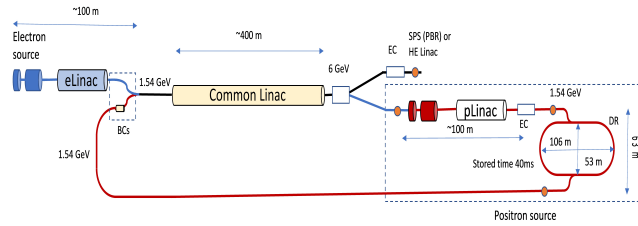


Figure 1: Layout of the FCC-ee pre-injector.

study. The final choice of the positron target will be made based on the estimated performances.

Conventional Target. Positron generation in conventional schemes is obtained through bremsstrahlung photons initiated by the incident electrons on an amorphous target and the photon conversion into electron-positron pairs in the same target. Reaching high conversion e^-/e^+ yields needs rather thick targets. In the case of the FCC-ee, the conversion target is made of an amorphous cylindrical piece of W. Two options are considered concerning the incident electron beam energy: 6 and 20 GeV. The target thickness for the 6 GeV case is of 17.5 mm.

Hybrid Target. The hybrid scheme [8] is based on the use of coherent radiation in an axially oriented mono-crystal as W. The high atomic potential (about 1 kV at normal temperature) for a $\langle 111 \rangle$ axially oriented W crystal allows the production of a high number of photons which conversion in an amorphous target provides also a high positron yield. In the case of the FCC-ee, the crystal is about 1 mm thick and the final parameters are under optimization studies. Between the two targets a dipole magnet rid off the charged particles emitted in the crystal may alleviate the heat load on the converter. Another option, permitted by the rather moderate intensities needed in the injector of a circular collider, consists in using a collimator between the two targets, reducing hence the incident photon spot size on the converter.

Targets and Materials Selection. Tungsten has rather good mechanical qualities. For bremsstrahlung photons and e^-/e^+ pairs its high-Z value provides high positron yield. Concerning the W crystal, a high-lattice potential is available at normal temperature (1 kV) and at low temperature (1.2 kV at 100 K). That allows a high photon radiation yield.

To avoid any early failures or damage of the target, experiments are planned to be conducted to test different materials for crystals and conversion targets at the values (PEDD) close to the ones expected at FCC-ee. The first feasibility test was performed at MAMI in fall 2021.

TARGET MATERIAL TESTS AT MAMI

Measurements at the MAMI B Facility

All the measurements discussed in this work were performed at the MAMI B facility. A scheme of the experimental hall is shown in Fig. 2. Measurements were performed

with low-emittance, high-intensity, 855 MeV electron beam on different samples at two positions along the beam path.

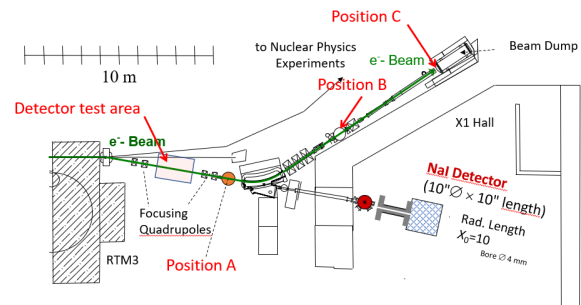


Figure 2: Floor plan at MAMI for X-ray and irradiation experiments.

Preliminary Results from Measurements at Point A

At the so-called point A, the beam was highly focused and a goniometer was available to remotely control the crystalline sample position and orientation with high precision. Downstream bending magnet has been used to separate the charged particles and the electromagnetic radiation emerging from the interactions of the electrons in the crystals. Thus, the integral energy spectrum of the latter was then measured by a NaI detector [9, 10]. The radiation spectra from some crystalline tungsten samples with high lattice quality were probed at point A. In particular, measurements in different beam-to-lattice relative orientations (in amorphous-like condition and along the $\langle 111 \rangle$ axis) and at different stages (at the beginning of the data taking session and after ~ 22.5 hours of irradiation with an 8-10 nA CW beam) were performed on a 1 mm thick, 8 mm \varnothing sample. Moreover, the angular range of the axial effects was probed by ionization chambers placed at an angle with respect to the beam nominal path: when in axial condition, the enhancement in electron scattering inside the sample corresponded to an increase in the current across the chambers. Thus, Fig. 3 shows the ratio between

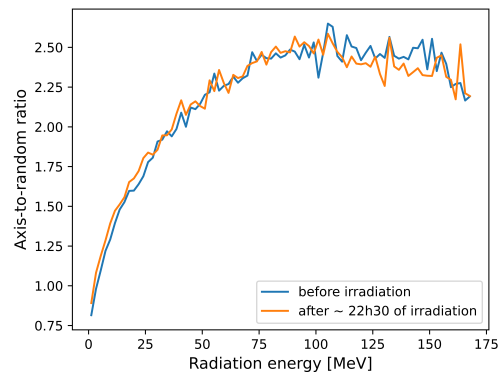


Figure 3: Ratio between the radiation spectra measured on axis and in random orientation before (blue) and after (orange) irradiating the 1 mm thick crystal.

the energy spectra of the electromagnetic radiation emerging

from the crystalline sample tested at point A, measured with a NaI detector. The orange (blue) curve was obtained before (after) the ~ 22.5 hour long irradiation. No differences have been observed between these two cases, which hints that the irradiation session didn't affect the sample lattice features noticeably. The latter can be clearly observed also in the goniometer scan data shown in Fig. 4: no significant variation in the width of the axial angular range has been found. In

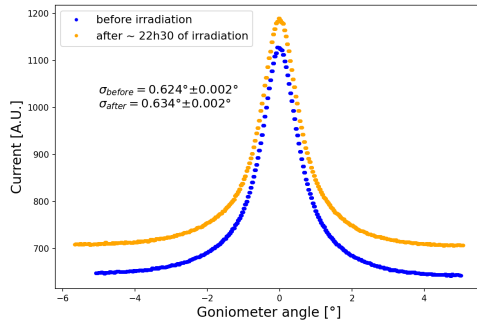


Figure 4: Ionisation chamber response as a function of the vertical goniometer angle. Angular scans were performed before (blue) and after (orange) irradiation. The width values printed on the figure were obtained by fitting each curve with a Gaussian.

this campaign, an overall fluence of $\sim 6.1 \times 10^{17} e^-/\text{mm}^2$ was obtained. During the full irradiation campaign, the electron beam size was monitored by using the wire scanning procedure. This was done by moving a metallic wire across the beam path at constant speed and measuring the current increase in the ionisation chambers, as it was done in the case of goniometer scans on the crystalline samples. Before and after the irradiation session, the beam size stayed at the rms values of $\sigma_x/\sigma_y = \sim 37/20 \mu\text{m}$.

Preliminary Results from Measurements at Point C

On the other hand, measurements of irradiation-induced heating and damage were performed at point C, i.e., at the beam dump (see Fig. 2), on different tungsten samples instrumented with thermocouples. K-type thermocouples were installed on the targets and read out by Ametek VTI Instruments EX1401 to measure the target steady state temperature and the temperature jump per pulse. An example of the raw data for different beam parameters is shown in Fig. 5. In particular, two targets were tested: a 2 mm thick, 8 mm \varnothing crystal (without orientation remote control) was irradiated for ~ 21 hours and a 2 mm thick, 50 mm \varnothing amorphous sample was irradiated for ~ 23 hours with 1-3 μA of average current pulsed beam. Fig. 6 shows the trends of the sample temperature, for both crystalline and amorphous tungsten, as a function of the irradiation time. The absolute temperature values reached during the irradiation sessions depend on the sample geometry and on the quality of the coupling with the thermocouples. Due to technical constraints, in the amorphous case, only the first ~ 6 hours of irradiation were actually monitored with the thermocouples, and there is a

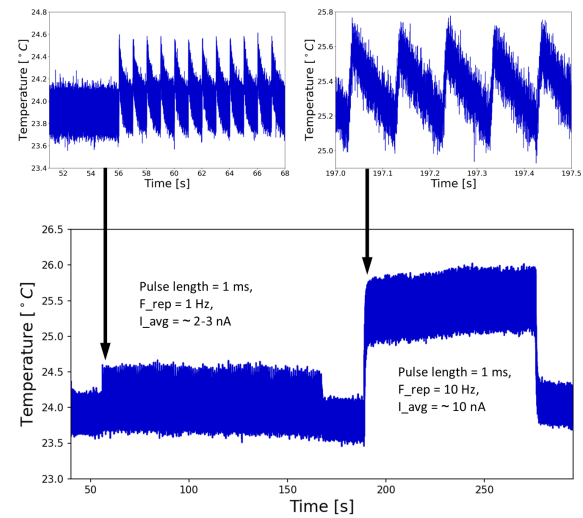


Figure 5: Commissioning of the data acquisition chain for the temperature measurements. Temperature as the function of time of the amorphous tungsten target installed at point C.

~ 3 hour long gap in the data acquired on the crystal. At

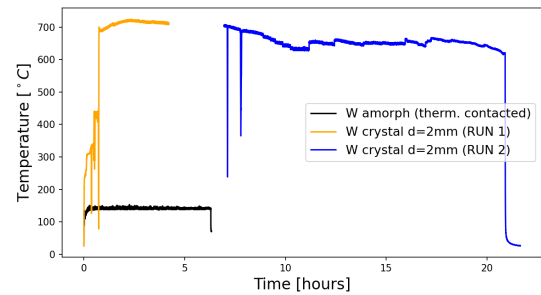


Figure 6: Temperature of the crystalline and amorphous tungsten samples installed at point C as a function of the irradiation time.

point C, no beam size monitoring was installed. As these values are crucial in order to simulate the target thermal load, an attempt was done to measure the beam size using the thermocouples having the size of $75 \mu\text{m}$, and found to be at the level of $\sigma_x/\sigma_y = \sim 330/230 \mu\text{m}$. The simulation studies (Geant4 and ANSYS) are under way to be compared with temperature measurements.

SUMMARY AND OUTLOOK

The first feasibility tests are very promising. The final conclusions will be drawn after targets are radiationally cooled and the detailed material analysis is performed. At position A, after 22.5 hours of irradiation, the coherent photon enhancement stayed the same as before with fluence of $\sim 6.1 \times 10^{17} e^-/\text{mm}^2$. ANSYS thermal simulations are under way to assess the target behavior during the beam tests. The next campaign is planned for this autumn to continue the irradiation tests (different target materials) with the improved set-up.

ACKNOWLEDGEMENTS

This publication is part of a project that has received funding from the European Union’s Horizon 2020 research and innovation programme under grant agreement STRONG – 2020 - No 824093. This work was supported by the ANR (Agence Nationale de la Recherche) under Grant No: ANR-21-CE31-0007 and partially financed by the INFN CSN1 (RD-MUCOL).

REFERENCES

- [1] M. Benedikt *et al.*, “Future Circular Collider: Conceptual Design Report Vol. 2”, accepted for publication in *EPJ ST*, CERN-ACC-2018-0057, 2018.
- [2] I. Chaikovska *et al.*, “Positron sources: from conventional to advanced accelerator concepts-based colliders”, *J. Instrum.* vol. 17, no. 5, pp. P05015, 2022. doi:10.1088/1748-0221/17/05/p05015
- [3] Y. Zhao *et al.*, “Optimisation of the FCC-ee Positron Source Using a HTS Solenoid Matching Device”, presented at the IPAC’22, Bangkok, Thailand, Jun. 2022, paper WEPOPT062, this conference.
- [4] X. Artru *et al.*, “Positron source using channeling in a tungsten crystal”, *Nucl. Instrum. Methods Phys. Res., Sect. A*, vol. 344, no. 3, pp. 443–454, 1994. doi:10.1016/0168-9002(94)90865-6
- [5] X. Artru *et al.*, “Radiation-Damage Study of a Monocrystalline Tungsten Positron Converter”, in *Proc. EPAC’98*, Stockholm, Sweden, Jun. 1998, paper MOP53C, pp. 1394–1396.
- [6] K. Oide *et al.*, “Design of beam optics for the future circular collider e^+e^- collider rings”, *Phys. Rev. Accel. Beams*, vol. 19, pp. 111005, 2016.
- [7] P. Craievich *et al.*, “The FCC-ee Pre-Injector Complex”, presented at the IPAC’22, Bangkok, Thailand, Jun. 2022, paper WEPOPT063, this conference.
- [8] X. Artru *et al.*, “Polarized and unpolarized positron sources for electron–positron colliders”, *Nucl. Instrum. Methods Phys. Res., Sect. B*, vol. 266, no. 17, pp. 3868–3875, 2008.
- [9] L. Bandiera *et al.*, “Investigation on radiation generated by sub-GeV electrons in ultrashort silicon and germanium bent crystals”, *Eur. Phys. J. C*, vol. 81, no. 284, 2021.
- [10] M. Soldani *et al.*, “Enhanced electromagnetic radiation in oriented scintillating crystals at the 100-MeV and sub-GeV scales”, *PoS*, vol. 853, EPS-HEP2021, 2022.